

60807
10/5/98

ATTITUDE AND TRAJECTORY ESTIMATION USING EARTH MAGNETIC FIELD DATA

Julie Deutschmann and Itzhack Bar-Itzhack¹
National Aeronautics and Space Administration
Goddard Space Flight Center
Greenbelt, Maryland 20771

Abstract

The magnetometer has long been a reliable inexpensive sensor used in spacecraft momentum management and attitude estimation. Recent studies have shown an increased accuracy potential for magnetometer-only attitude estimation systems. Since the earth's magnetic field is a function of time and position, and since time is known quite precisely, the differences between the computed and measured magnetic field components, as measured by the magnetometers throughout the entire spacecraft orbit, are a function of both the spacecraft trajectory and attitude errors. Therefore, these errors can be used to estimate both trajectory and attitude. Traditionally, satellite attitude and trajectory have been estimated with *completely separate systems*, using different measurement data. Recently, trajectory estimation for low earth orbit satellites was successfully demonstrated in ground software using only magnetometer data. This work proposes a *single augmented Extended Kalman Filter* (EKF) to simultaneously and autonomously estimate both spacecraft trajectory and attitude with data from a magnetometer and either dynamically determined rates or gyro-measured body rates.

I. Introduction

The magnetometer, due to its reliability and low cost, has been the focus of many studies in the recent past. Emphasis has been placed on using the magnetometer alone, without any additional input, to estimate the spacecraft trajectory (References 1, 2, and 3) and attitude (References 4 and 5). Studies have also been performed to determine the ultimate accuracy of the magnetometer in estimating attitude when accurate rate information is available (Reference 6).

In using the magnetometer to estimate attitude, the spacecraft position is required to compute the reference magnetic field. In using the magnetometer to estimate position, including the spacecraft attitude improves the results. The data used to estimate either the position or the attitude is a function of the difference between the observed magnetometer measurements and the reference magnetic field. In this work we use this difference to estimate *both* the spacecraft attitude and position. This is an extension of the work performed by Shorshi and Bar-Itzhack (Reference 1) to add the attitude to the trajectory state vector.

Many of the future missions, such as the Small and Mid-size Explorer Series and university class explorers, are looking for low cost and autonomous approaches to navigation and attitude estimation. This work could prove valuable to these missions as a prime navigation system, with coarse accuracy requirements, or a backup to a prime system where more stringent accuracy is required.

In this work we present the method of expanding the Extended Kalman Filter of Reference 1 to include the estimation of the spacecraft attitude, and the results of tests on the combined filter using simulated data. Incorporating the attitude into the filter requires an estimate of the rates. In this work we assume that the

¹ Sophie and William Shamban Professor of Aerospace Engineering, Faculty of Aerospace Engineering, Technion-Israel Institute of Technology, Haifa 32000 Israel, Currently at NASA GSFC as an NRC NASA Research Associate.

rates would be provided by gyroscopes. A method similar to that of Challa (Reference 4) or Azor, Bar-Itzhack, and Harman (Reference 7) could be applied, though, in the absence of gyroscope data.

II. Extended Kalman Filter Algorithm

The EKF algorithm is based on the following assumed models:

$$\text{System Model:} \quad \dot{\underline{X}} = \underline{f}(\underline{X}(t), t) + \underline{w}(t) \quad (1)$$

$$\text{Measurement Model:} \quad z_k = \underline{h}_k(\underline{X}(t_k)) + \underline{v}_k \quad (2)$$

where $\underline{w}(t)$ is a zero mean white process, \underline{v}_k is a zero mean white sequence, and $\underline{X}(t)$ is the state vector defined as

$$\underline{X}^T = [a, e, i, \Omega, \omega, \theta, C_d, \underline{q}]$$

The first six elements of $\underline{X}(t)$ are the classical Keplerian elements which determine the spacecraft position and velocity, namely the semi-major axis (a), eccentricity (e), inclination (i), right ascension of the ascending node (Ω), argument of perigee (ω), and true anomaly (θ). C_d is the drag coefficient and \underline{q} represents the attitude quaternion.

Measurement Update Stage:

The linearization of equation (2) results in

$$z_k = H_k \underline{X}_k + v_k \quad \text{where } H_k = [H_o \mid H_a] \quad (3)$$

H_o is the measurement matrix for the orbital states and is derived in Reference 1, and H_a is the measurement matrix for the attitude states. The derivation of H_a is given in Appendix A. The effective measurement used by the filter is given as

$$z_k = \underline{B}_{m,k} - \hat{\underline{B}}(\hat{\underline{X}}_k, t_k) \quad (4)$$

where $\underline{B}_{m,k}$ is the magnetic field vector measured by the magnetometer and $\hat{\underline{B}}(\hat{\underline{X}}_k, t_k)$ is the estimated magnetic field vector as a function of the estimated state $\hat{\underline{X}}_k$ at time t_k . The dependence of $\hat{\underline{B}}(\hat{\underline{X}}_k, t_k)$ on the position and the attitude is seen in the derivation of equation (3) in Appendix A.

The state update equation is

$$\hat{\underline{X}}_k(+) = \hat{\underline{X}}_k(-) + K_k z_k \quad (5)$$

where K_k is the Kalman gain computed according to

$$K_k = P_k(-) H_k^T [H_k P_k(-) H_k^T + R_k]^{-1} \quad (6)$$

R_k is the measurement noise matrix and the covariance matrix is updated as usual with

$$P_k(+) = [I - K_k H_k] P_k(-) [I - K_k H_k]^T + K_k R_k K_k^T \quad (7)$$

Equation (5) is used to update the orbital states, but not the attitude states. The update of the attitude states is done as follows. As shown above, the state vector contains the attitude represented by a quaternion. The

EKF estimates an error in the quaternion, expressed as a vector of three small angles, $\underline{\alpha}$, defined in Appendix A and derived in Reference 8. This error is combined with the current estimate of the quaternion to give an updated estimate of the quaternion, which is then propagated to the next time point.

Propagation Stage:

The *filter* dynamics model is given as

$$\underline{X}'_{k+1} = A_k(\underline{X}'_k) \underline{X}'_k + \begin{bmatrix} w_o \\ w_a \end{bmatrix} \quad \text{where} \quad A_k(\underline{X}'_k) = \begin{bmatrix} A_o & 0 \\ 0 & A_a \end{bmatrix} \quad (8)$$

where $\underline{X}'^T = [a, e, i, \Omega, \omega, \theta, C_d, \underline{\alpha}]$

A_o is the linearized transition matrix for the orbital states and is a function of the *estimated* orbital states, which are elements of \underline{X}' . A_o is defined in Reference 9. A_a is the transition matrix for the attitude error, $\underline{\alpha}$, which are also included in \underline{X}' . A_a is based on the development from Reference 8. The transition matrices A_o and A_a are first order approximations computed from the Jacobian $F_k(\underline{X}_k)$ derived from the linearization of equation (1).

The covariance matrix is propagated from time t_k to time t_{k+1} using:

$$P_{k+1}(-) = A_k(\hat{\underline{X}}'_k(+)) P_k(+) A_k(\hat{\underline{X}}'_k(+))^T + Q_k \quad (10)$$

Q_k is the process noise covariance matrix for both the orbit and attitude states. The orbit states are propagated by solving equation (1) numerically without the noise component, as in Reference 8. The dynamics of the attitude states is linear. Assuming a constant angular velocity between gyro measurements, the attitude states are propagated using

$$\hat{\underline{q}}_{k+1}(-) = \Phi_k \hat{\underline{q}}_k(+) \quad (11)$$

where

$$\Phi_k = I + \Psi_k T + \frac{1}{2!} (\Psi_k T)^2 + \frac{1}{3!} (\Psi_k T)^3 + \frac{1}{4!} (\Psi_k T)^4 + \frac{1}{5!} (\Psi_k T)^5 + \dots \quad (12)$$

and

$$\Psi_k = 0.5 \begin{bmatrix} 0 & w(3) & -w(2) & w(1) \\ -w(3) & 0 & w(1) & w(2) \\ w(2) & -w(1) & 0 & w(3) \\ -w(1) & -w(2) & -w(3) & 0 \end{bmatrix} \quad \text{and } \underline{w} = \underline{w}_k$$

T is the time between gyro measurements, \underline{w} is the angular velocity vector, and the arguments 1, 2, 3 refer to the 3 components of \underline{w} . Equations (10) through (12) are particularly suitable when testing with simulated data, because the rates are almost constant, with added noise. When the filter is applied to real data, equation (1) will be solved numerically without the noise component, as in Reference 8.

III. Simulation

A basic simulation was developed to test the EKF outlined above. The scenario consisted of simulating a spacecraft in low-earth-orbit with an earth-pointing attitude, i.e. maintaining a one revolution-per-orbit (RPO) attitude. The spacecraft axes, or body axes, are aligned with the orbital axes as defined in Figure 1.

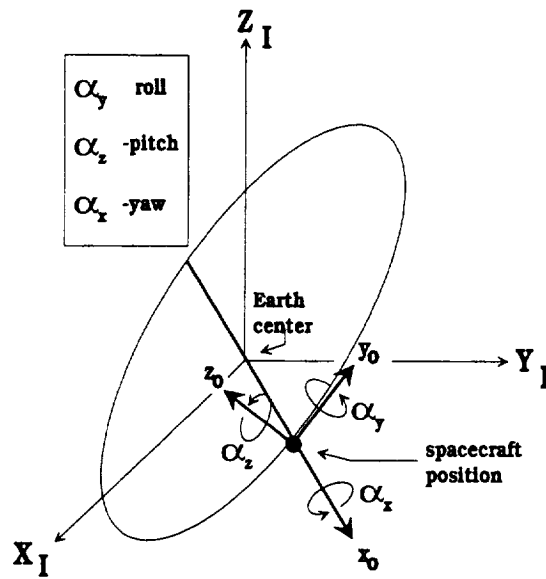


Figure 1. Definition of Orbital Axes

The rotation rate, \underline{w} , used in equation (11), has a component only about the z_0 axis. The derivation of the instantaneous rate experienced by the spacecraft is given in Appendix B. The axes labeled with 'I' refer to the inertial coordinate system. Those marked with 'o' refer to the orbital coordinates. The quaternion represents the rotation from inertial coordinates to body coordinates. The attitude error, $\underline{\alpha}$, represents three small Euler angles around the body coordinates, which rotate the estimated quaternion to the true quaternion. The attitude displayed in the table below and in the results section is given in terms of Euler angles also. These Euler angles describe the attitude with respect to the orbital coordinates. Euler angles were chosen for the display since the true Euler angles are all zero.

The parameters which define the baseline simulated orbit and attitude are given below.

<u>Parameter</u>	<u>Truth</u>	<u>A-priori estimate</u>
a (km)	7000	8000
e	0.05	0.06
i (deg)	50	54
Ω (deg)	90	85
ω (deg)	0	5
θ (deg)	45	50
C_d	0.02	1
roll (deg)	0	10
pitch (deg)	0	10
yaw (deg)	0	10

IV. Results

The simulation described above was run for 300,000 seconds. Noise was added to the simulated magnetometer data and to the simulated rate data. The magnetometer measurement noise was 2 milliGauss and the noise in the measured rate was $0.017 \text{ deg/sec}^{1/2}$.

Figures 2 through 4 show the root-sum-square (RSS) error in the position estimate. The a-priori position error is 1453 km (computed from the orbital parameters given above). Figure 2 shows the error for the entire 300,000 seconds, approximately 51 revolutions (the orbital period is 97 minutes). Figure 3 shows the first 20,000 seconds. The error converges to less than 100 km within 10,000 seconds, which is roughly 1.7 orbits. Figure 4 shows the final 50,000 seconds. The average converged position error is about 4 km.

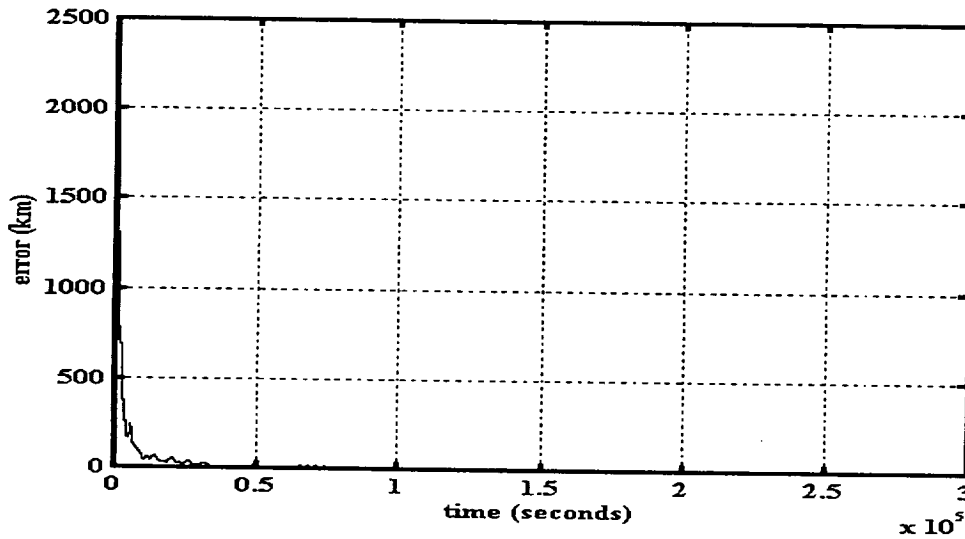


Figure 2. RSS Position Error

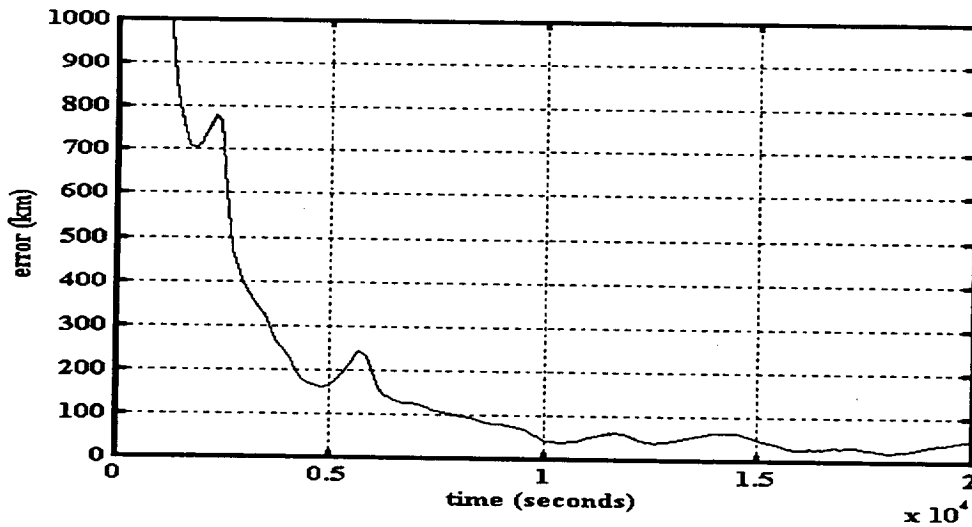


Figure 3. RSS Position Error - First 20,000 Seconds

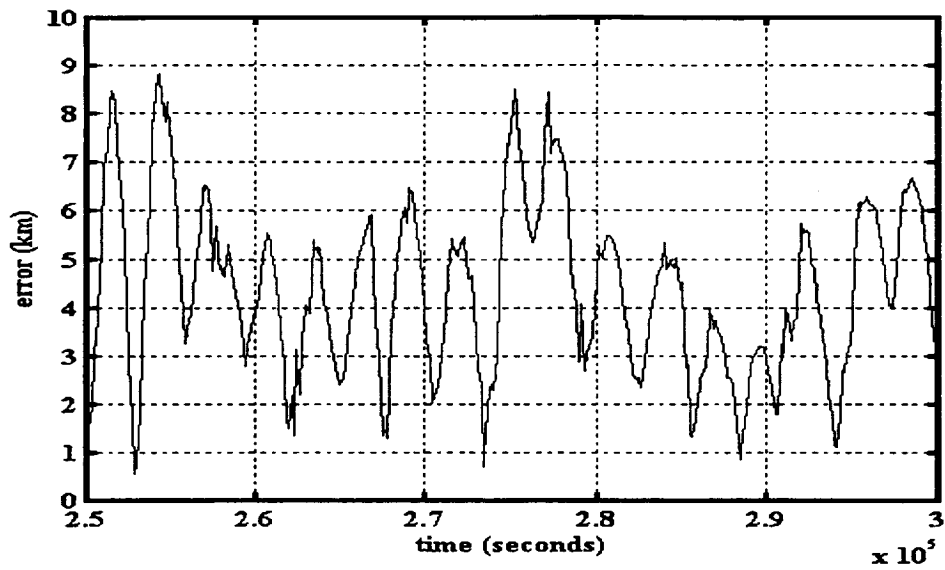


Figure 4. RSS Position Error - Last 50,000 Seconds

Figures 5 through 7 show the RSS attitude error. The attitude converges quickly, to less than 5 degrees, within 3,000 seconds as shown in Figures 5 and 6. Figure 7 shows that the average steady state error is less than 1 degree.

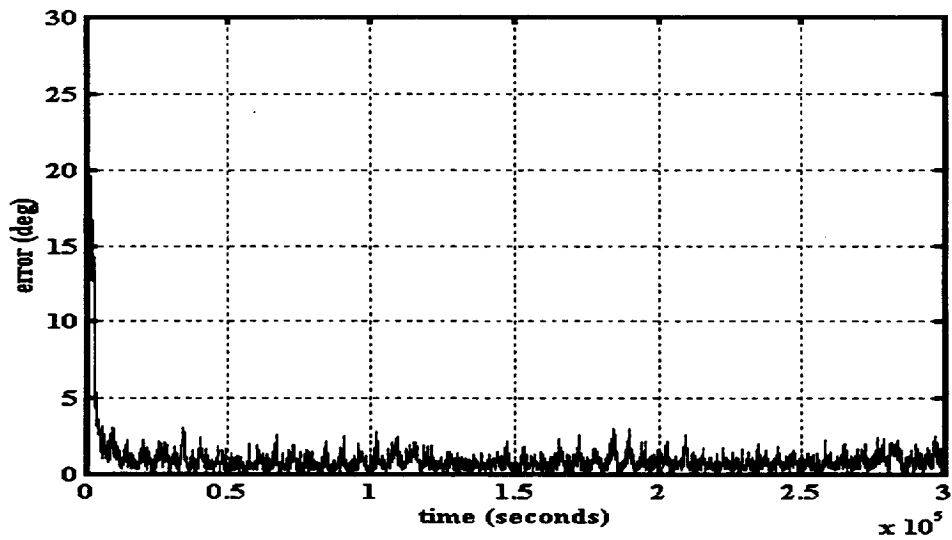


Figure 5. RSS Attitude Error

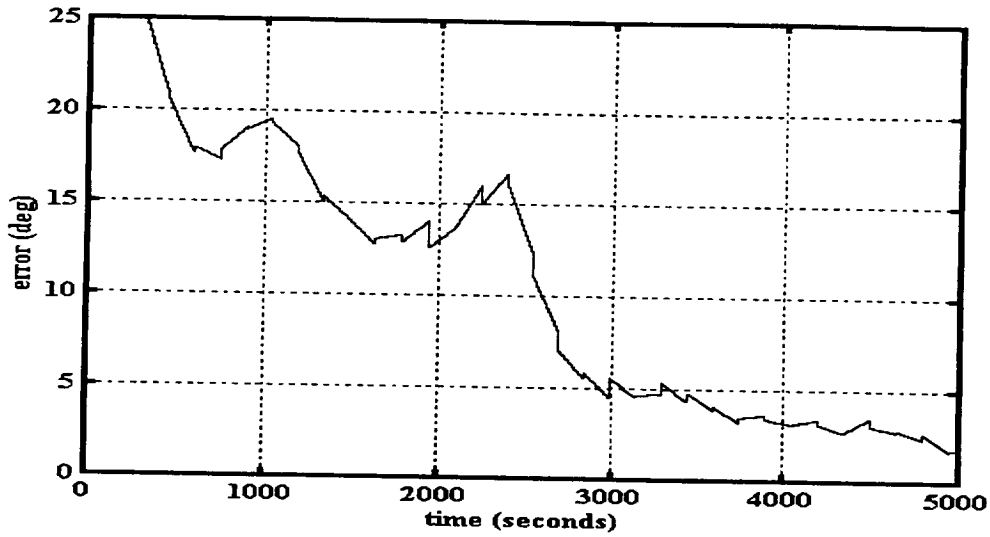


Figure 6. RSS Attitude Error - First 5,000 seconds

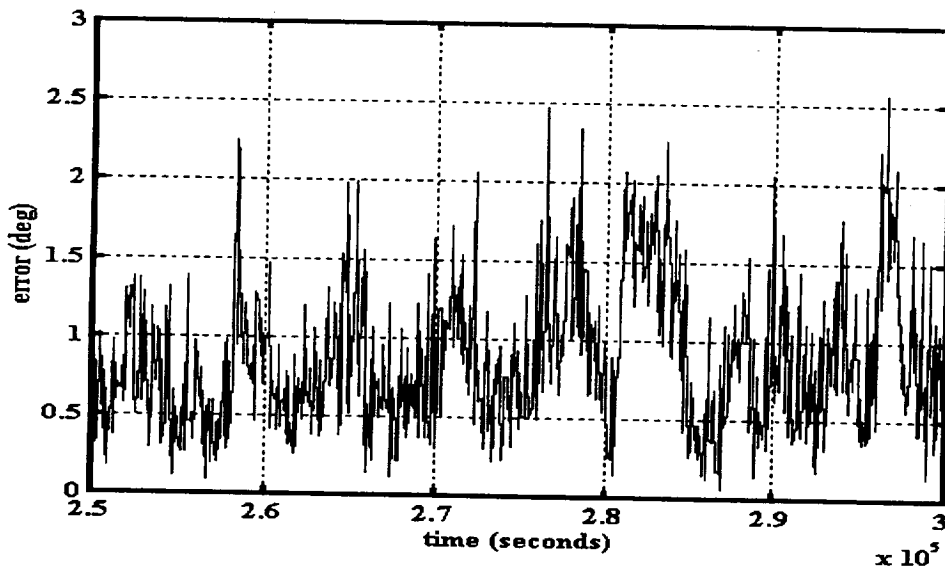


Figure 7. RSS Attitude Error - Last 50,000 Seconds

Figures 8 through 10 show the RSS velocity error. The a-priori velocity error is 0.96 km/sec. Like the position, the velocity error converges within 10,000 seconds, as shown in Figure 8. Figure 9 shows that the error is less than 0.25 km/sec at the end of the first 5,000 seconds. Figure 10 shows that the steady state velocity error is approximately 0.004 km/sec.

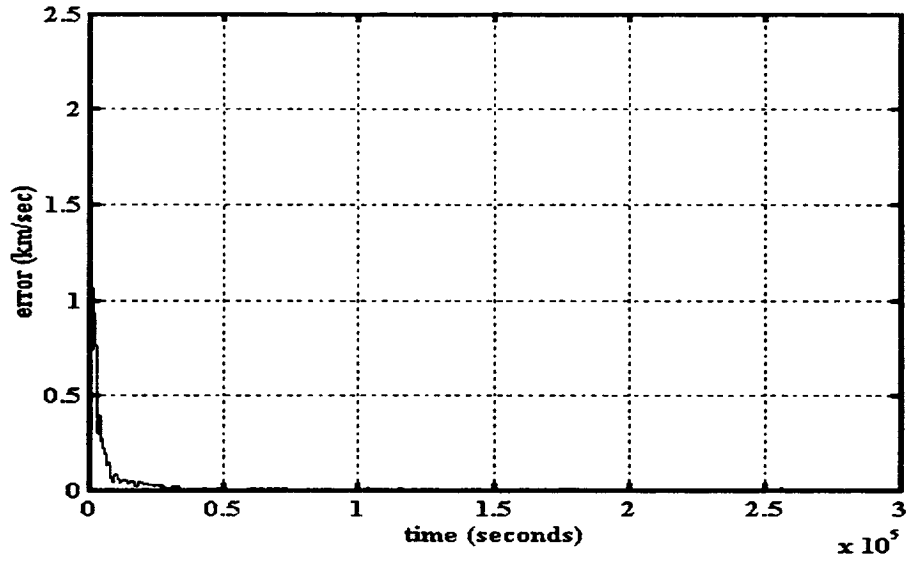


Figure 8. RSS Velocity Error

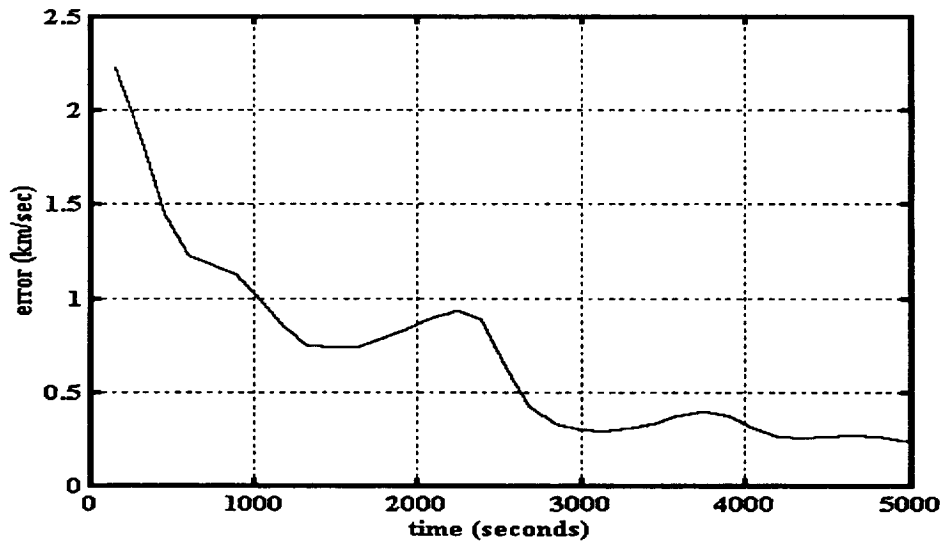


Figure 9. RSS Velocity Error - First 5000 Seconds

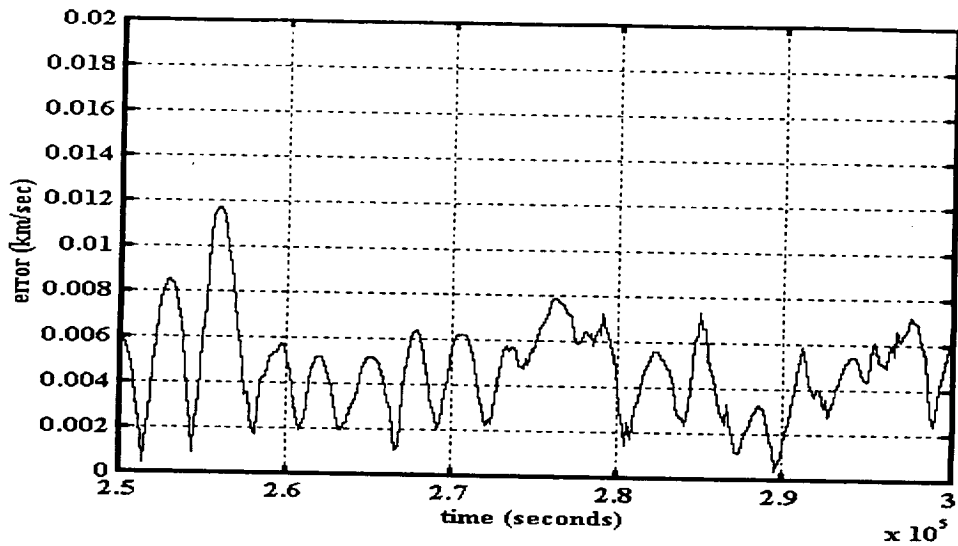


Figure 10. RSS Velocity Error - Last 50,000 Seconds

Figure 11 shows the RSS measurement residuals for the first 70,000 seconds (the residuals are computed using equation (4)). The average value is approximately 4 milliGauss. The residuals also converge quickly from an initial value of 186 milliGauss (RSS).

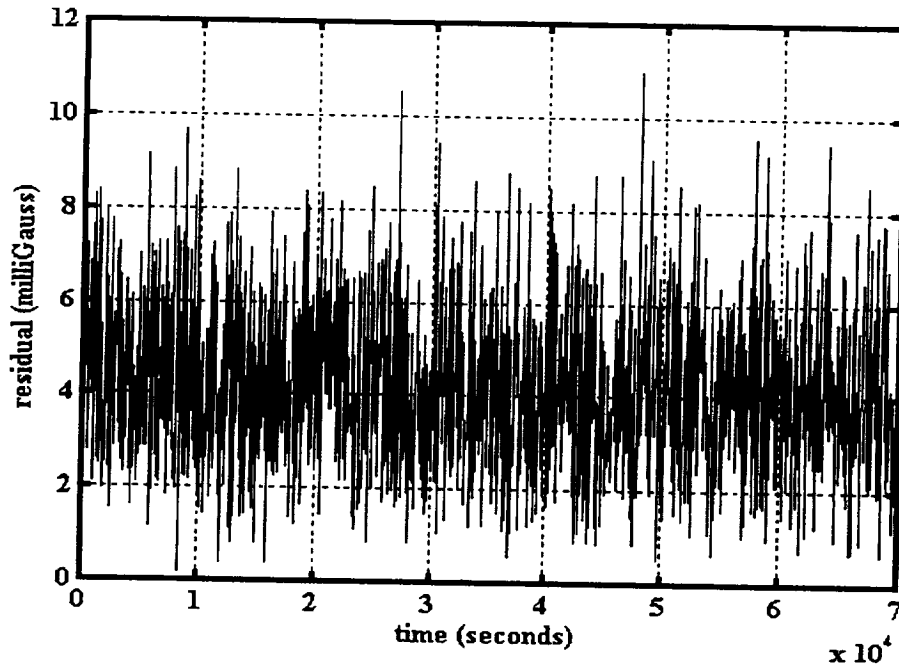


Figure 11. RSS Residual

V. Conclusions and Future Work

This work presents a *single augmented Extended Kalman Filter* that simultaneously estimates both spacecraft trajectory and attitude using data from magnetometers and gyroscopes. The results from the first test of this filter using simulated data, indicate that the filter can indeed estimate both the trajectory and attitude. Starting with errors (RSS) of over 1400 km in position and 10 degrees in attitude, the filter converged to less than 5 degrees in attitude within 3,000 seconds and to less than 100 km in position in 10,000 seconds (1.7 orbits). The average steady state values are less than 1 degree for attitude and 4 km for position. The steady state velocity errors (RSS) are approximately 4 m/sec and the average magnetometer residual is about 4 milliGauss (RSS).

Further testing will be conducted both with simulated and real spacecraft data. The magnetic field varies more at higher inclinations. Therefore, the effect of the orbit inclination angle will be studied. Tests will be conducted as to the filter's ability to estimate attitude and trajectory at low inclinations. The sensitivity to errors in Ω will be examined. Shorshi and Bar-Itzhack (References 1 and 9) found that the estimation of Ω was critical to the convergence of the position error. Additional errors will be introduced into the simulated data, e.g. magnetometer and gyro biases. The state vector will be expanded to include these biases and the ability of the filter to estimate these added states will be tested. Finally, tests with real spacecraft data from satellites such as the Gamma Ray Observatory, the Upper Atmospheric Research Satellite, and the Extreme Ultraviolet Explorer will be conducted.

References

1. Shorshi, G. , and Bar-Itzhack, I., "Satellite Autonomous Navigation Based on Magnetic Field Measurements", *Journal of Guidance, Control, and Dynamics*, Vol. 18, No. 4, July-August, 1995, pp. 843-850.
2. Ketchum, E., "Autonomous Spacecraft Orbit Determination Using the Magnetic Field and Attitude Information", Paper No. AAS 96-005, presented at the 19th Annual AAS Guidance and Control Conference, Breckenridge, Colorado, February 1996.
3. Psiaki, M., "Autonomous Orbit and Magnetic Field Determination Using Magnetometer and Star Sensor Data", *Journal of Guidance, Control, and Dynamics*, Vol. 18, No. 3, May-June 1995, pp. 584-592.
4. Challa, M., Natanson, G., Deutschmann, J., and Galal, K., "A PC-Based Magnetometer-Only Attitude and Rate Determination System for Gyroless Spacecraft", Paper No. 07, presented at the GSFC FDD Flight Mechanics/Estimation Theory Symposium 1995, NASA Goddard Space Flight Center, Greenbelt, Maryland, May 16-18, 1995.
5. Martel, F., Pal, P., and Psiaki, M., "Three-Axis Attitude Determination via Kalman Filtering of Magnetometer Data", presented at the GSFC FDD Flight Mechanics/Estimation Theory Symposium 1988, NASA Goddard Space Flight Center, Greenbelt, Maryland, May 10-11, 1988.
6. Hashmall, J., Liu, K., and Rokni, M., "Accurate Spacecraft Attitudes from Magnetometer Data", Paper No. MS95/007, presented at the CNES International Symposium on Space Dynamics, Toulouse, France, June 19-23, 1995.
7. Azor, R., Bar-Itzhack, I., and Harman, R., "Satellite Angular Rate Estimation from Vector Measurements", presented at the GSFC FDD Flight Mechanics/Estimation Theory Symposium 1996, NASA Goddard Space Flight Center, Greenbelt, Maryland, May 14-16, 1996.

8. Deutschmann, J., Bar-Itzhack, I., and Rokni, M., "Comparison and Testing of Extended Kalman Filters for Attitude Estimation of the Earth Radiation Budget Satellite", presented at the GSFC FDD Flight Mechanics/Estimation Theory Symposium 1990, NASA Goddard Space Flight Center, Greenbelt, Maryland, May 22-24, 1990.
9. Shorshi, G. and Bar-Itzhack, I., "Satellite Autonomous Navigation Based on Magnetic Field Measurements", TAE No. 714, Technion-Israel Institute of Technology, Haifa, Israel, April 1994
10. Kaplan, M., *Modern Spacecraft Dynamics & Control*, John Wiley & Sons, New York, 1976.

APPENDIX A - Derivation of the Measurement Model

The magnetic field vector can be resolved in the magnetic spherical coordinates, as shown in Figure A.1, as $\underline{B}_F^T = [B_r, B_{\theta B}, B_{\phi B}]$.

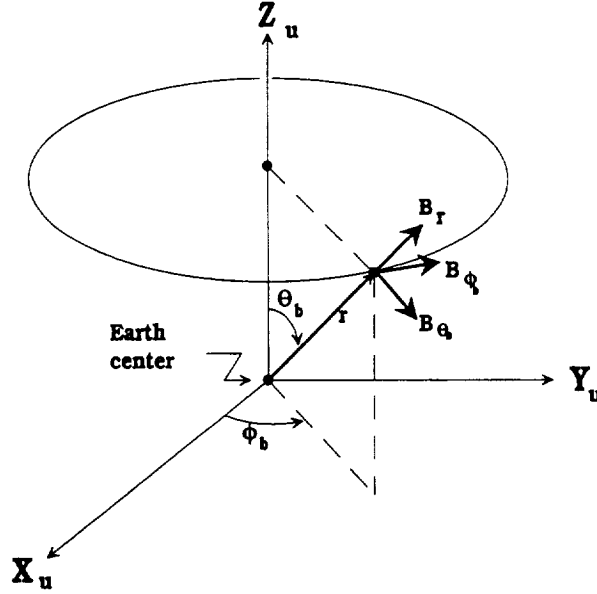


Figure A.1. Definition of the Magnetic Spherical Coordinates

The magnetic field at the spacecraft location, computed using the IGRF magnetic field model and the estimated position, can be written as

$$\hat{\underline{Y}} = \hat{D}_b^I \hat{D}_I^F \hat{\underline{B}}_F + \underline{n}' \quad (\text{A.1})$$

and the measured magnetic field vector, as measured by the magnetometer can be written as

$$\underline{Y}_m = D_b^I D_I^F \underline{B}_F + \underline{n}_m \quad (\text{A.2})$$

where

- D_b^I = the transformation from inertial to body coordinates
- D_I^F = the transformation from magnetic spherical to inertial coordinates
- \underline{n}' = the magnetic field model error
- \underline{n}_m = the magnetometer measurement error

The effective measurement, z , is defined as follows

$$z = \underline{Y}_m - \hat{\underline{Y}} = D_b^I D_I^F \underline{B}_F + \underline{n}_m - \hat{D}_b^I \hat{D}_I^F \hat{\underline{B}}_F - \underline{n}' \quad (\text{A.3})$$

Rewriting the transformation of $\hat{\underline{B}}_F$ as

$$\hat{D}_b^I \hat{D}_I^F \hat{B}_F = D_b^I D_I^F B_F + \Delta(D_b^I D_I^F B_F) \quad (\text{A.4})$$

and

$$\underline{n} = \underline{n}_m - \underline{n}' \quad (\text{A.5})$$

This leads to

$$\underline{z} = \Delta(D_b^I D_I^F B_F) + \underline{n} \quad (\text{A.6})$$

where

$$\Delta(D_b^I D_I^F B_F) = \Delta D_b^I (D_I^F B_F) + D_b^I \Delta(D_I^F B_F) \quad (\text{A.7})$$

The second term on the right hand side of equation (A.7) is the derivation of the measurement matrix for the orbital states given in Reference 9. The expansion of the first term leads to the measurement matrix for the attitude states. Rewriting that term as

$$\Delta D_b^I (D_I^F B_F) = \Delta D_b^I B_I \quad (\text{A.8})$$

where

B_I = the computed magnetic field vector in inertial coordinates

The error in the transformation can be defined as the difference between the true body coordinates and an intermediate coordinate system, referred to as the computed body coordinate system. The matrix that is computed is \hat{D}_b^I , which is equivalent to a transformation to the computed body coordinate system, which can be written as

$$\hat{D}_b^I = D_c^I = D_c^b D_b^I \quad (\text{A.9})$$

so

$$\Delta D_b^I = D_c^b D_b^I - D_b^I \quad (\text{A.10})$$

where D_b^I is the true transformation from inertial to body coordinates. For small attitude error we can assume that the matrix D_c^b is composed of small angles, thus

$$D_c^b = I - \begin{bmatrix} 0 & -\psi & \vartheta \\ \psi & 0 & -\phi \\ -\vartheta & \phi & 0 \end{bmatrix} = I - [\alpha \ x] \quad (\text{A.11})$$

therefore from equation (A.11)

$$\Delta D_b^I = I - [\alpha \ x] D_b^I - D_b^I = -[\alpha \ x] D_b^I \quad (\text{A.12})$$

Substituting equation (A.12) into the first term on the right-hand side of equation (A.7) yields

$$\Delta D_b^I (D_1^R B_F) = -[\underline{\alpha} \ x] D_b^I \cdot B_1 = -[\underline{\alpha} \ x] B_b = [B_b \ x] \underline{\alpha} \quad (A.13)$$

Substituting equation (A.13) into equation (A.6) along with the measurement matrix for the orbital states, gives

$$z = [B_b \ x] \underline{\alpha} + H_o x_o + \underline{n} = [H_o \ [B_b \ x]] \underline{x} + \underline{n} \quad (A.14)$$

where H_o is the measurement matrix for the orbital states, x_o , and \underline{x} is composed of both the orbital states and the small angular errors in the attitude, $\underline{\alpha}$. Since B_b is not known, the magnetic field vector measured by the magnetometer is used instead. The combined measurement matrix is then given as

$$H = [H_o \ [B_b \ x]] = [H_o \ H_a] \quad (A.15)$$

APPENDIX B - Derivation of Spacecraft Rotation Rate

The instantaneous rotation rate about the spacecraft z_o is derived here from the orbital parameters which

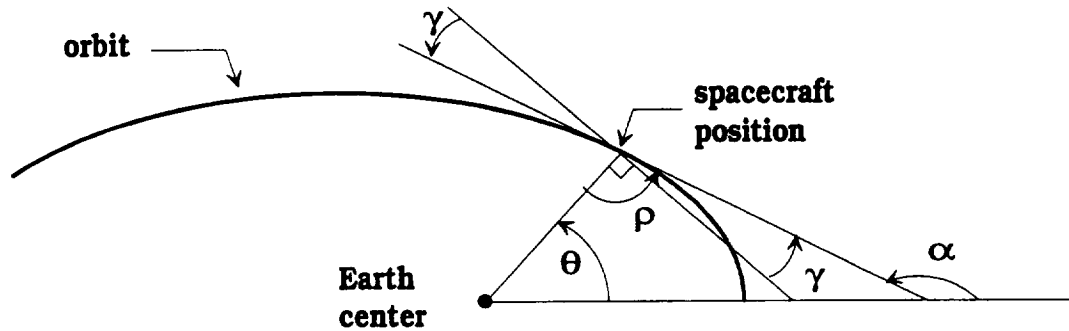


Figure B.1. Relationship Between Orbital Angles

describe an elliptical orbit (the average rate is 1 RPO). Figure B.1 defines the angles α , ρ , z , and γ . The rotation rate, w_z , is defined as

$$w_z = \dot{\alpha} \quad (B.1)$$

The angle, α , can be written as

$$\alpha = \theta + \rho \quad (B.2)$$

but

$$\rho = \pi / 2 + \gamma \quad (\text{B.3})$$

therefore

$$\alpha = \theta + \pi / 2 + \gamma \quad (\text{B.4})$$

Equation (B.1) then becomes

$$w_z = \dot{\alpha} = \dot{\theta} + \dot{\gamma} \quad (\text{B.5})$$

The relationship between the Keplarian elements, e , θ , and γ is given as (Reference 10)

$$\tan(\gamma) = \frac{e \cdot \sin(\theta)}{1 + e \cdot \cos(\theta)} \quad (\text{B.6})$$

then

$$\frac{d}{dt} \tan(\gamma) = \frac{d}{dt} \left[\frac{e \cdot \sin(\theta)}{1 + e \cdot \cos(\theta)} \right] \quad (\text{B.7})$$

Performing the differentiation in equation (B.7) leads to the following equation

$$w_z = \dot{\theta} - \frac{\cos^2(\gamma)}{1 + e \cdot \cos(\theta)} \left[\frac{e^2 \cdot \sin^2(\theta) \dot{\theta}}{1 + e \cdot \cos(\theta)} + e \cdot \cos(\theta) \dot{\theta} \right] \quad (\text{B.8})$$

